Adaptive Control of a Lower-Limb Prosthesis Using a Momentum Observer and PSO-Based Gain Optimization

Original Scientific Paper

Ahmed Qaftan Kafi*
University of Technology,
College of Control and Systems Engineering,
cse.23.17@grad.uotechnology.edu.iq

Muayed Sadik Croock
University of Technology,
College of Electrical Engineering,
muayad.s.croock@uotechnology.edu.iq

Qusay Fadhil Hasan
University of Technology,
College of Control and Systems Engineering,
qusay.f.hasan@uotechnology.edu.iq

*Corresponding author

Abstract *– The number of individuals who live with limb loss has increased worldwide. Individuals with limb loss face significant daily challenges in independent mobility and functional activities. A primary technical barrier in modern active prostheses is the effective management of Ground Reaction Force (GRF), which introduces unpredictable disturbances during the gait cycle and complicates control due to nonlinear dynamics. This research addresses the need for a control framework that can simultaneously compensate for unknown GRF-related disturbances and manage nonlinear prosthetic dynamics. The study proposes an adaptive control framework for a 2-Degree-of-Freedom (DOF) lower-limb prosthesis, integrating a computed-torque-based adaptive controller with a generalized momentum observer for GRF estimation. To enhance performance, Particle Swarm Optimization (PSO) was employed to tune the controller and observer gains, replacing traditional trial-and-error methods. Simulations were conducted in MATLAB/SIMULINK using realistic disturbances derived from the GAITREC GRF dataset. Results demonstrate that PSO-based tuning significantly improved tracking accuracy, reducing Root Mean Square (RMS) tracking errors by 47% at the knee and 94% at the ankle compared to manual tuning. Additionally, GRF estimation errors were reduced by 57% and 48% for the knee and ankle, respectively. Comparative analysis shows that the proposed PSO approach provides superior global search capabilities and convergence stability over previous bio-inspired methods such as the Bat Algorithm(BA). While the framework offers a robust, data-independent solution for various locomotion scenarios, it is currently limited by its simplified 2-DOF model and lack of real-time validation. Future research should focus on implementing the controller in physical hardware to verify its performance and safety in real-world environments.*

Keywords*: Lower limb prosthesis, adaptive control, PSO optimization, disturbance observer, ground reaction force, Lyapunov theory*

Received: January 21, 2026; Received in revised form: May 6, 2026; Accepted: May 6, 2026

1. INTRODUCTION

The estimated population of individuals living with limb loss in the United States was 2,309,000, 91% of whom had lower extremity amputation. This number is expected to rise by 145% in 2060 [1]. The loss of a limb caused substantial daily challenges, particularly in independent mobility and performing basic functional activities. These difficulties have driven extensive research efforts aimed at developing prosthetic limbs capable of movements that align closely with the user's intended actions [2, 3].The control of lower-limb prostheses remains a significant challenge due to dynamic nonlinearity, uncertainty, and the effect of external forces, especially ground reaction force GRF which causes external disturbances that are difficult to pre-

dict or measure directly due to changes in gait, terrain, and load while accommodating the device's complex interaction with the human body. These challenges highlight the need for control strategies that can reject disturbances caused by external forces during the gait cycle [4, 5]. Modern lower-limb prostheses can generally be classified into passive, semi-active, and active (powered) systems[6]. Passive prostheses have fixed mechanics and cannot adapt to different gait conditions, which often limit their function [7]. Semi-active devices use microprocessors to control their damping and stiffness for better adaptability; however, because they do not produce positive mechanical power, their effectiveness is limited for demanding activities like climbing stairs [8]. Active or powered prostheses overcome these limitations by employing actuators that inject energy into the gait cycle. As a result, they enable more natural joint motion, improved stability, and greater functional independence benefits that are highly important for individuals with transfemoral amputation [9]. Many control strategies proposed to enhance the performance of lower limb powered prosthesis these methods can be classified in to two level: the first level that rely in sensors that are used to detect the movement using pattern recognition technique, and the second level includes the techniques that seek to enhance tracking performance under uncertainty and external disturbance [10]. However, achieving high-performance control in such systems remains a challenge because prosthetic joints exhibit nonlinear dynamics, parameter uncertainty, and strong interaction with the user and environment. In particular, GRF introduces significant external disturbances during the stance phase, and these disturbances vary continuously with gait phase, terrain, walking speed, and loading conditions [11–13].

A review of previous studies shows that considerable effort has been devoted to improving prosthetic control under uncertainty. Boucetta *et al*. [14] proposed an adaptive control approach that considers the interaction between the prosthesis and the ground. An Adaptive Takagi–Sugeno (TS) Fuzzy–PID controller was used for trajectory tracking, where the fuzzy inference system determines the gait phase using femur–tibia angles and GRF components, while the PID controller minimizes the position error. Simulation results showed improved tracking performance under different conditions; however, the study was limited to only three locomotion modes. Salman and Kadhim [15] Developed an optimal Backstepping Controller to address nonlinearity and parameter uncertainty in 2-DOF, The authors employed the BA, a bio-inspired optimization method, to automatically adjust the controller parameters, Simulation results showed that the BA-optimized controller achieved notable improvements, reducing tracking error by 9% for the first joint and 7.4% for the second joint, while preserving strong robustness against external torque disturbances but consider no the external forces, GRF is not modeled, measured, or estimated. Peixoto *et al*. [16] focused on state estimation using a variable high-gain observer to avoid direct velocity measurement, showing stable performance under noise and parameter uncertainty; however, the work mainly addressed observer design rather than explicit compensation of stance-phase GRF effects. More recently, Pi [17] introduced a concurrent adaptive control framework with human-in-the-loop optimization to improve gait personalization and comfort, where electromyography (EMG) signals were used to estimate the effect of GRF. Based on the above review, an important research gap remains. There is still a need for a control framework that can simultaneously address nonlinear prosthetic dynamics, compensate for unknown GRF-related disturbances during the stance phase. This issue is important because insufficient disturbance compensation can degrade tracking accuracy, reduce gait stability, and limit the practical deployment of powered prostheses in real-world environments. Therefore, improving disturbance-aware control is not only a theoretical requirement but also a practical necessity for safer and more reliable assistive devices.

To address this gap, this paper proposes an adaptive control framework for a 2-DOF lower-limb prosthesis that combines a computed-torque-based adaptive controller, a generalized momentum observer, and PSO-based gain tuning. In the proposed method, the generalized momentum observer is used to estimate GRF while PSO is employed to optimize key controller and observer gains for improved tracking and disturbance rejection. In this way, the proposed approach integrates model-based adaptation, observer-based disturbance estimation, and optimization-based tuning into a unified control structure.

2. DYNAMIC MODEL

The powered lower-limb prosthesis considered in this study is modeled as a planar 2-DOF robotic mechanism representing the knee and ankle joints. The dynamic equations of motion are derived using the classical Euler–Lagrange formulation widely used in robotic manipulators and prosthetic systems. Let $q=[q_1, q_2]^T$ denote the ankle and knee joint angles. The motion of the system is governed by the nonlinear joint-space equation

$$M\ddot{q} + C\dot{q} + G = \tau + \tau_d \tag{1}$$

$$\begin{bmatrix} M_{11}(q) & M_{12}(q) \\ M_{21}(q) & M_{22}(q) \end{bmatrix} \ddot{q} + \begin{bmatrix} C_{11}(q,\dot{q}) & C_{12}(q,\dot{q}) \\ C_{21}(q,\dot{q}) & C_{22}(q,\dot{q}) \end{bmatrix} \dot{q} \begin{bmatrix} g_1(q) \\ g_2(q) \end{bmatrix} = \begin{bmatrix} \tau_d \\ \tau_d \end{bmatrix} + \begin{bmatrix} \tau_1 \\ \tau_2 \end{bmatrix}$$

where $M(q) \in R^{2\times2}$ is the inertia matrix, $C(q, q^{\cdot}) \in R^{2\times2}$ represents Coriolis and centrifugal effects, $G(q) \in R^2$ denotes the gravitational torques, τ is the actuator input, and τ_d The external disturbances caused by GRF. The components of the above equation are given by

$M_{11}=m_1 d_1^2+ I_1+I_2+m_2 (l_1^2+d_2^2+2l_1 l_2 cosq_2)$

$M_{12}=m_2 d_2^2+I_2+m_2 l_2 d_2 \cos q_2$

$M_{21}=m_2 d_2\text{^}2+I_2+ m_2 l_2 d_2 cosq_2$

$M_{22}=m_2 d_2^2+I_2$

$C_{11}= -m_2 l_1 d_2 sinq_2 q^{\cdot}_2$, $C_{12}=-m_2 l_1 d_2 sinq_{-2}(q^{\cdot}_1+q^{\cdot}_2)$

$C_{21}=m_2 l_1 d_2^{\cdot} sinq_2 q_1^{\cdot}$

$C_{22}=0$

$G_1 = m_1 d_1 gcosq_1 + m_2 g(d_2 cos(q_1+q_2)+l_1 cosq_1)$,

$G_2=m_2 d_2 gcos(q_1+q_2)$.

where each term depends on the link masses m_i, moments of inertia I_i, center-of-mass distances d_i, and segment lengths, the system parameters are described in the Table.1 , (Fig.1) precent the a schematic diagram of the dynamic model.

The external torque is related to the cartesian GRF through the well-known Jacobian-transpose mapping [18]:

$$\tau_d = J(q)^T Fe \tag{2}$$

Where $J(q)$ The Jacobian matrix is described as below:

$$J(q)=\begin{bmatrix} -l_1 \sin q_1 - l_2 \sin(q_1+q_2) & -l_2 \sin(q_1+q_2) \\ l_1 \cos q_1 + l_2 \cos(q_1+q_2) & l_2 \cos(q_1+q_2) \end{bmatrix} \tag{3}$$

The following properties characterize for the dynamic system [19]:

Property 1. The inertia matrix $M(q)$ is symmetric and positive, which is further bound:

$$\lambda_1 \|x^2\| < x^T M(q) x < \lambda_2 \|x^2\|, \forall x, \theta \in R^n, \tag{4}$$

where $\alpha 1$ and $\alpha 2$ are the positive constants and ‖. ‖ is the standard Euclidean norm.

Property 2. The centrifugal and Coriolis matrix $C(q, \dot{q}) \in R^{2\times 2}$ and the time derivative of the inertia matrix $\dot{M}(q) \in R^{2\times 2}$ satisfy the following equation:

$$x^T [\dot{M}(q) - 2C(q, \dot{q})] x = 0 \tag{5}$$

Property 3. The uncertain term τ_d is limited by a positive constant δ as follows:

$$|\tau_d| < \delta \tag{6}$$

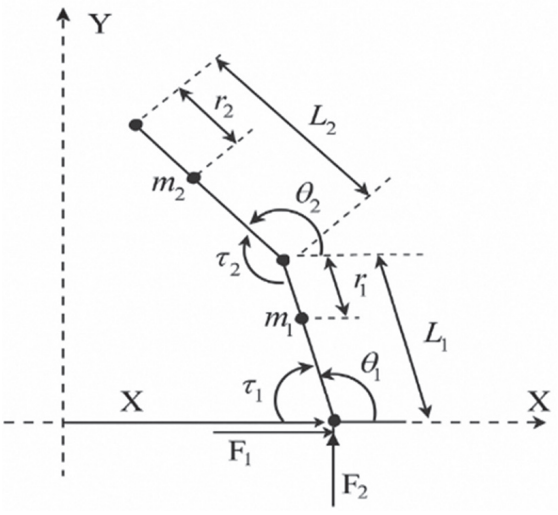

Fig.1. Schematic diagram of prosthesis model

To simulate the prosthetic lower limb model representation by using Eq.1, Table 1 exhibits the model parameters values that utilized in the simulation.

Table 1. Physical parameters of the system

Parameter	Description	Value	Unit
m_1	shank mass	1.5	kg
m_2	foot mass	3.0	kg
l_1	shank length	0.22	m
l_2	foot length	0.15	m
I_1	inertia of link 1	1.3	kg·m²
I_2	inertia of link 2	1.9	kg·m²
r_1	Distance to the center of mass(link1)	0.17	m
r_2	Distance to the center of mass(link2)	0.15	m
g	gravitational acceleration	9.81	m/s²

3. CONTROL DESIGN

3.1. OBSERVER DESIGN

To estimate the unknown disturbance, torque τ_d a momentum-based observer is formulated. The generalized momentum and its corresponding time derivative are defined as [20]:

$$p = M(q)\dot{q} \tag{7}$$

$$\dot{q} = \dot{M}\dot{q} + M\ddot{q} \tag{8}$$

The dynamic model Eq. (1) can be expressed in terms of the generalized coordinates as:

$$M\ddot{q} = -C\dot{q} - G + \tau + \tau_d \tag{9}$$

Substituting the dynamics from above into the momentum derivative yields:

$$p^{\cdot} = \tau + \tau_d - Cq^{\cdot} - g + M^{\cdot}q^{\cdot} \tag{10}$$

By utilizing the property 2 results:

$$p^{\cdot} = \tau + \tau_d + C^T q^{\cdot} - g \tag{11}$$

A residual signal r designed to track the disturbance:

$$r = K_O(p - \int_0^t (\tau + C^T q^{\cdot} - g + r)ds - p(0)) \tag{12}$$

where $p(0)$is the initial value of the generalized momentum and K_O

$$K_O = \text{diag}(k_{O,i}) > 0$$

The time derivative of the residual satisfies:

$$\dot{r} = -K_O(r - \tau_d) \tag{13}$$

which shows that r converges exponentially to the unknown disturbance torque:

$$\hat{\tau_d} = r \tag{14}$$

3.2. ADAPTIVE CONTROL DESIGN

The adaptive controller ensures that the actual joint motion q accurately tracks the reference trajectory q_r despite uncertainties in the system model and unknown disturbance. The tracking error and it is derivative defined by:

$$e = q - q_r \tag{15}$$

$$\dot{e}=\dot{q}-\dot{q}_r \quad (16)$$

To stabilize the tracking error, a filtered error surface is introduced:

$$s=\dot{e}+\Lambda e \quad (17)$$

where Λ is a diagonal positive-definite gain matrix. Consequently, the reference velocity $\dot{q_r}$, and acceleration $\ddot{q_r}$ are defined as:

$$\dot{q_r}=\dot{q_d}-\Lambda e \Rightarrow \dot{q}=s+q_r \quad (18)$$

$$\ddot{q_r}=(\ddot{q_d}=-\Lambda\dot{e} \Rightarrow \ddot{q}=\dot{s}+(\ddot{q_r}) \quad (19)$$

Substituting the expressions for $\dot{q}$and $\ddot{q}$ into the system dynamics Eq. (1) yields:

$$M(q)(\dot{s}+(\ddot{q_r})+C(q,\dot{q})(s+(\dot{q_r})+G(q)=\tau_d+\tau \quad (20)$$

Rearranging the terms to isolate the manifold dynamics:

$$M(q)\dot{s}+C(q,\dot{q})s=\tau-[M(q)(\ddot{q_r}+C(q,\dot{q})\dot{q}_r+G(q)]-\tau_d \quad (21)$$

The manipulator dynamics admit a linear parameterization [21] in terms of the unknown inertial parameters, expressed as

$$M(q)\ddot{q}_r + C(q,\dot{q})\dot{q}_r + G(q) = Y(q,\dot{q},\dot{q}_r,\ddot{q}_r) \quad (22)$$

Substituting this into Eq. (21) yields

$$M(q)\dot{s} + C(q,\dot{q})\,s = \tau - Y(q,\dot{q},\dot{q}_r,\ddot{q}_r)\theta - \tau_d \quad (23)$$

The adaptive control law is chosen as:

$$\tau = Y(q,\dot{q},\dot{q}_r,\ddot{q}_r)\,\hat{\theta} - K_D s + \widehat{\tau_d} \quad (24)$$

where $\hat{\theta}$ represents the estimated parameters, K_D is a positive-definite feedback gain, and $\hat{\tau_d}$ is the estimated disturbance using a momentum observer. The parameter estimates are updated according to the adaptation law:

$$\dot{\hat{\theta}} = -\Gamma\, Y^T(q,\dot{q},\dot{q}_r,\ddot{q}_r)\, s \quad (25)$$

where Γ is a positive definite adaptation gain matrix. This formulation ensures robustness to parameter uncertainties and allows the controller to compensate for unknown external disturbances.

3.3. STABILITY ANALYSIS

To study the convergence properties, a Lyapunov candidate function is chosen as

$$V = \frac{1}{2}s^T M(q)s + \frac{1}{2}\widetilde{\theta^T}\Gamma^{-1}\tilde{\theta} \quad (26)$$

$$\dot{V} = s^T M\dot{s} + \tfrac{1}{2}s^T\dot{M}s + \widetilde{\theta^T}\Gamma^{-1}\dot{\tilde{\theta}} \quad (27)$$

$$\dot{V} = s^T\left(-Cs + Y\tilde{\theta} - K_D s + \tau_d\right) + \tfrac{1}{2}s^T\dot{M}s + \widetilde{\theta^T}\Gamma^{-1}\dot{\tilde{\theta}} \quad (28)$$

$$\dot{V} = -s^T K_D s + s^T Y\tilde{\theta} + \widetilde{\theta^T}\Gamma^{-1}\dot{\tilde{\theta}} + s^T\tau_d \quad (29)$$

$$\dot{V} = -s^T K_D s + \underbrace{s^T Y\tilde{\theta} - \widetilde{\theta^T}Y^T s}_{0} + s^T\tau_d \quad (30)$$

$$\dot{V} = -s^T K_D s + s^T\tau_d$$

To analyze the stability under Property 3, we use the norm properties:

$$\dot{V} \le -\lambda_{min}(K_D)||s||^2 + ||s|| \cdot ||\tau_d||$$

$$\dot{V} \le -||s||(\lambda_{min}(K_D)||s|| - \delta)$$

For $\dot{V}$ to be strictly negative $\dot{V} < 0$ the following condition must hold:

$$||s|| > \frac{\delta}{\lambda_{min(K_D)}}.$$

The stability proof confirms that the system is Uniformly Ultimately Bounded (UUB). Because of the uncertain term τ_d, the tracking error s may not reach zero, but it is guaranteed to stay within a small, predictable range around it.

3.4. PARTICULAR SWARM OPTIMIZATION (PSO)

The PSO method, a prominent category of swarm intelligence for addressing optimization problems and finding both local and global solutions, was first introduced by Kennedy and Eberhart in 1995 [22]. The PSO algorithm involves three main stages: generating particle positions and velocities, updating velocities, and updating positions. This approach is inspired by the behavior of some animals [23, 24].The velocity of the particle in each iteration is computed by [25]

$$V_i^{k+1}=w\cdot V_i^k+C_1\cdot_{rand}\cdot(p_{best}-X_i^k)+C_2\cdot rand\cdot(g_{best}-X_i^k) \quad (31)$$

where the weights w , C_1 and C_2 are, respectively, the inertia, p_{best}, personal best which represents the best position previously achieved by the *i* particle, while g_{best} global best represents the best position found by the entire swarm, the function "rand" generates random numbers with zero mean, and the inertia weight can be given by

$$w = w_{\max} - (w_{\max} - w_{\min})k/k_{\max} \quad (32)$$

Where k is the current number of iterations, k_{max} is the maximum number of iterations, w_{max} and w_{min} are the maximum and minimum weights, respectively. The position updated by[25].

$$X_i^{k+1} = X_i^k + V_i^{k+1} \quad (33)$$

where X_i^k and X_i^{k+1} indicate the current and updated values of the particles, which represent the chosen design parameters to be tuned , the cost function selected to minimize the integral of time-weighted absolute error (ITAE).

$$cost = \int_0^T t\cdot|e|\,dt \quad (34)$$

4. SIMULATION AND RESULT

The optimized adaptive based momentun observer controller designed for lower limb prosthesis to stablization, traking, GRF estimation. A MATLABR2025b/ SIMULINK was used for simulation and analyze the performance of the controller. The simulations were

carried out using the ode45 variable-step solver, with a maximum step size of 1e−3 s to ensure numerical stability and accurate dynamic response. The initial joint angles and velocities were set to zero. the RMSE has been chosen as a metric for evaluating performance. The PSO algorithm was employed to tune the design parameters. The PSO convergence behavior, shown in. (Fig. 2), indicates rapid descent of the cost during the first eight iterations, followed by near-complete saturation, confirming that the selected optimization parameters ensured stable and reliable convergence. The swarm was initialized with 20 particles over 25 iterations, utilizing an inertia weight of 0.7 and acceleration coefficients 1.5. The optimal values of the controller design parameters, with the lower and upper bounds, are listed in Table 2, while the flowchart of the PSO optimization process is shown in Fig. 3

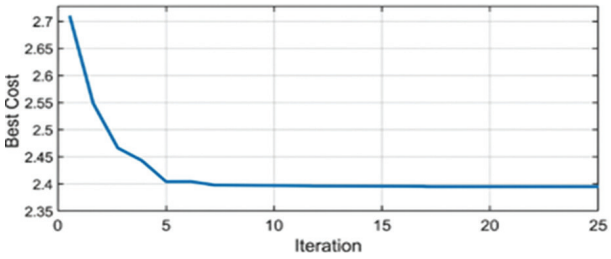

Fig. 2. PSO algorithm convergence curve

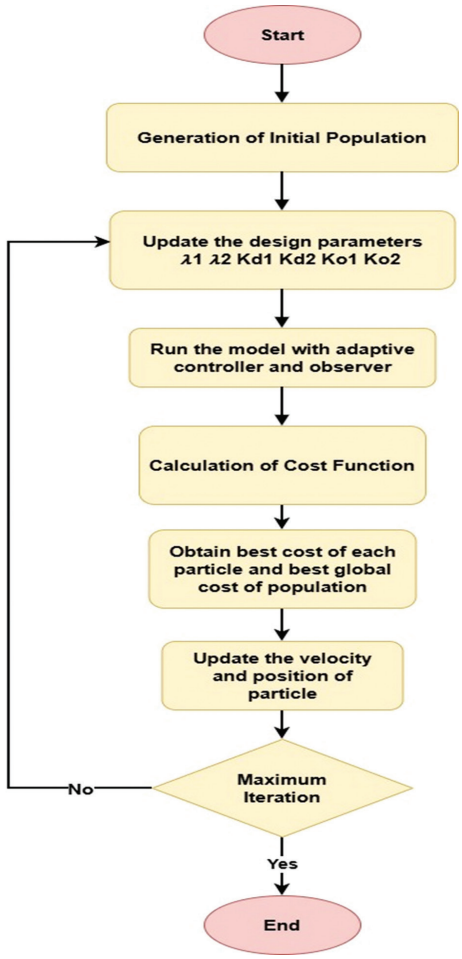

Fig. 3. Flowchart of the PSO optimization process

Table 2. Optimized parameters with corresponding bounds

Design Parameters	Min	Max	Optimal value
$\lambda 1$	5	20	12
$\lambda 2$	5	20	10
K_{d1}	10	30	20
K_{d2}	10	30	15
K_{o1}	20	80	60
K_{o2}	20	80	40

The performance of the proposed control architecture was evaluated using a nonlinear 2-DOF leg model subjected to realistic disturbances derived from the GAITREC GRF dataset [26] From this database, the vertical (Fz) and anterior–posterior (Fx) GRF components of the right leg were extracted from a representative stance-phase trial. These forces were time-aligned and interpolated to match the simulation sampling rate, then transformed into joint-space disturbances using a simple moment-arm relation, to maintain physical consistency and prevent actuator saturation, the resulting torques were scaled by 0.094 at the knee and 0.092 at the ankle. Fig. 4 present the original GRF signals extracted from the GAITREC dataset prior to scaling and joint-space transformation, illustrating the characteristic loading profile of the human stance phase.

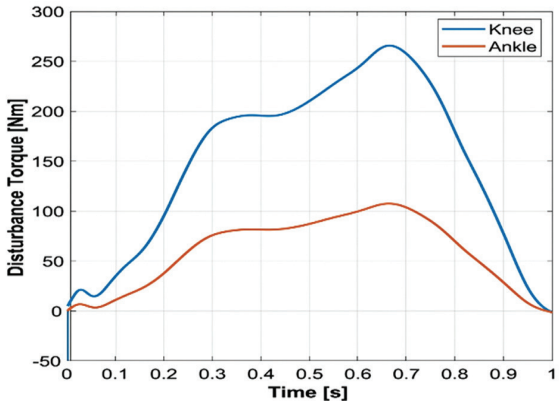

Fig. 4. GRF signals

Fig. 5 and Fig. 6 presents the performance of both the controller and the observer when the design parameters are manually tuned using trial-and-error, while Fig. 7, Fig. 8, Fig. 9, show the tracking performance, GRF estimation, and control signal, respectively, after tuning the design parameters using PSO.

The controller exhibited significantly improved tracking performance after optimization. The RMS tracking error of the knee joint was reduced by approximately 47%, while the ankle joint RMS error reduced by 94%. In addition, the estimation error of the GRF disturbance was reduced by approximately 57% in the knee joint and 48% in the ankle joint, Furthermore, the control effort remained within acceptable physiological and mechanical limits, with no saturation or high-frequency oscillations (Fig 8). The average torque magnitudes

for the optimized controller were approximately 17.7 Nm for the knee and 5.6 Nm for the ankle, confirming that the improved accuracy was not achieved at the expense of excessive control energy Overall, the optimized controller exhibits highly accurate tracking, robust GRF estimation, and stable behavior under realistic loading conditions. These results confirm the effectiveness of the proposed momentum-observer-based control structure during the stance phase.

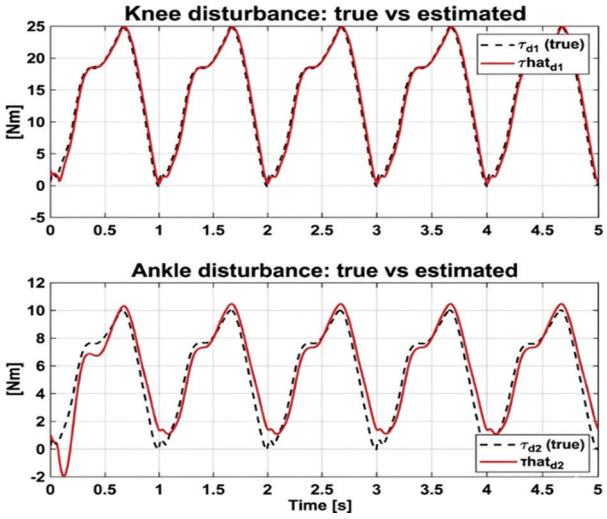

Fig. 5. Estimated GRF disturbances at the knee and ankle Joints

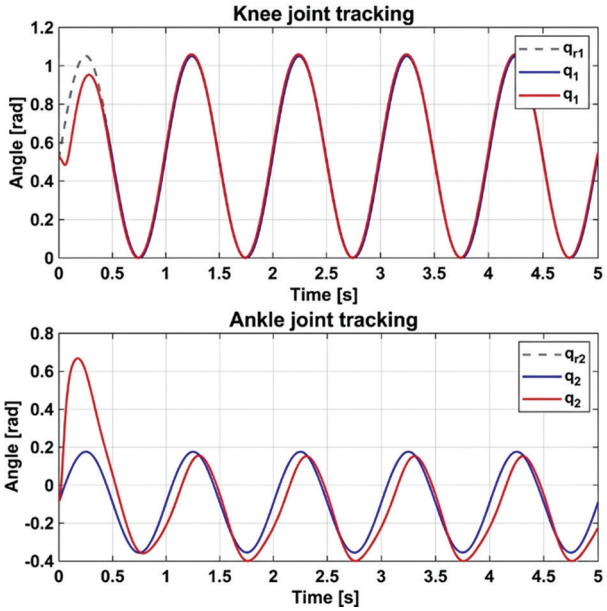

Fig. 6. Tracking performance of knee and ankle joints using tri and error

The proposed method demonstrates superior performance compared with previous work. The comparison includes the optimization algorithm, the GRF estimation method, and the range of motion. The proposed controller achieved better trajectory tracking in both knee and ankle position compared with Salman and Kadhim's [15], while the BA-optimized backstepping controller reduced the errors by 9% and 7.4% for the first and second joints, respectively, the PSO approach reduces errors by 47% and 94% for those links. Furthermore, unlike the method proposed by Boucetta *et al*. [14], was limited to three locomotion modes and requires a dataset to estimate GRF, and Pi [17] was utilized EMG to estimate the GRF, which needs sensor, and the signal itself inherently noisy. The proposed structure employs a momentum observer for this purpose. Despite these improvements, the study remains limited by its simplified 2-DOF model and simulation only without real-time validation.

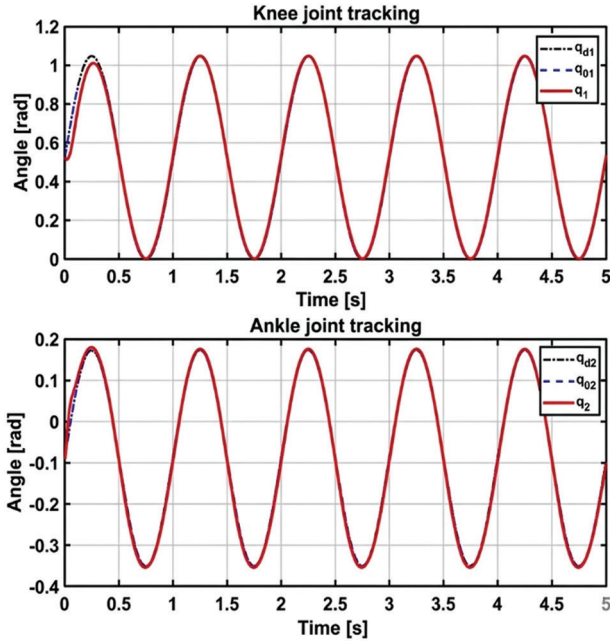

Fig. 7. Tracking performance of knee and ankle joints using tri and PSO

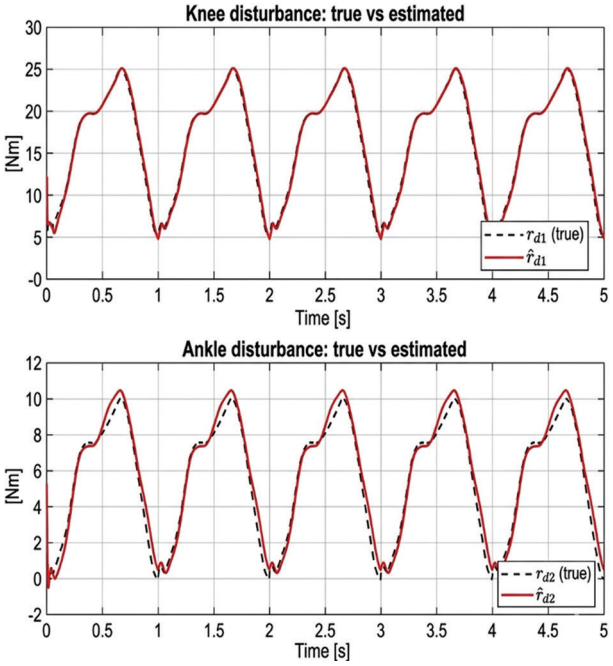

Fig .8. Estimated GRF disturbances at the knee and ankle joints after optimization

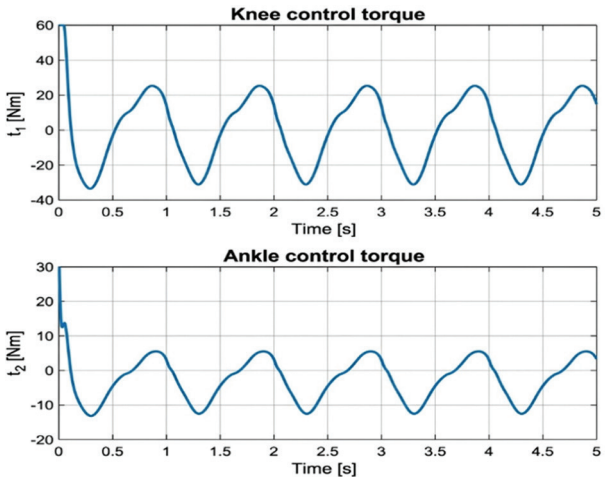

Fig. 9. Knee and ankle joint torques

5. CONCLUSION

This study presented a design and developed a 2-DOF lower limb prosthesis control farmwork using the adaptive-based Lyapunov approach, with a momentum observer to estimate GRF during the stance phase. The performance of the proposed controller has been verified by simulation on MATLAB 2025Rb. The PSO algorithm was used to tune the parameters of both the controller and observer. The proposed controller with PSO results showed that the tracking performance of both knee and ankle was improved by 47% and 94%, respectively, compared with the tri and error method and compared with the BA algorithm used in previous work. In addition, the estimation error of the GRF disturbance was enhanced by approximately 57% in the knee joint and 48% in the ankle joint.

DECLARATION OF THE USE OF AI TOOLS

The authors used Grammarly for language editing, grammar checking, and improving the clarity of the manuscript. All AI-assisted content was reviewed and edited by the authors, who take full responsibility for the integrity and accuracy of this work. No AI tool is listed as an author, and AI tools are not cited as primary sources

REFERENCE:

[1] J. A. Rivera, K. Churovich, A. B. Anderson, B. K. Potter, "Estimating Recent US Limb Loss Prevalence and Updating Future Projections", Archives of Rehabilitation Research and Clinical Translation, Vol. 6, No. 4, 2024, p. 100376. doi: 10.1016/j.arrct.2024.100376

[2] B. Yuan, D. Hu, S. Gu, S. Xiao, F. Song, "The global burden of traumatic amputation in 204 countries and territories", Frontiers in Public Health, Vol. 11, 2023, p. 1258853. doi: 10.3389/FPUBH.2023.1258853

[3] A. Domínguez-Ruiz, E. O. López-Caudana, E. Lugo-González, F. J. Espinosa-García, R. Ambrocio-Delgado, U. D. García, R. López-Gutiérrez, M. Alfaro-Ponce, P. Ponce, "Low limb prostheses and complex human prosthetic interaction: A systematic literature review", Frontiers in Robotics and AI, Vol. 10, 2023, p. 1032748. doi: 10.3389/FROBT.2023.1032748

[4] S. L. Phillips, L. Resnik, C. Fantini, G. Latlief, "Endpoint control for a powered shoulder prosthesis", Journal of Prosthetics and Orthotics, Vol. 25, No. 4, 2013, pp. 193-200. doi: 10.1097/JPO.0000000000000006

[5] H. A. Mansour, H. N. Abdullah, "Design and Implementation of Remote Evaluation System for the Prosthetic Limbs", Proceedings of the 3rd International Conference for Emerging Technology, Belgaum, India, 27-29 May 2022. doi: 10.1109/INCET54531.2022.9824666

[6] C. F. Pană, L. F. Manta, I. C. Vladu, Ș. I. Cismaru, F. L. P. Besnea, D. Cojocaru, N. Bîzdoacă, "The Design of a Smart Lower-Limb Prosthesis Supporting People with Transtibial Amputation—A Data Acquisition System", Applied Sciences, Vol. 12, No. 13, 2022. doi: 10.3390/APP12136722

[7] R. Gehlhar, M. Tucker, A. J. Young, A. D. Ames, "A review of current state-of-the-art control methods for lower-limb powered prostheses", Annual Reviews in Control, Vol. 55, 2023, pp. 142-164. doi: 10.1016/J.ARCONTROL.2023.03.003

[8] Z. Zhang, H. Yu, W. Cao, X. Wang, Q. Meng, C. Chen, "Design of a Semi-Active Prosthetic Knee for Transfemoral Amputees: Gait Symmetry Research by Simulation", Applied Sciences, Vol. 11, No. 12, 2021. doi: 10.3390/APP11125328

[9] L. Flynn, J. Geeroms, R. Jimenez-Fabian, S. Heins, B. Vanderborght, M. Munih, R. Molino Lova, N. Vitiello, D. Lefeber, "The Challenges and Achievements of Experimental Implementation of an Active Transfemoral Prosthesis Based on Biological Quasi-Stiffness: The CYBERLEGs Beta-Prosthesis", Frontiers in Neurorobotics, Vol. 12, 2018. doi: 10.3389/FNBOT.2018.00080

[10] X. Ma, X. Zhang, J. Xu, "Robotic Leg Prosthesis: A Survey From Dynamic Model to Adaptive Control for Gait Coordination", IEEE Transactions on Neural Systems and Rehabilitation Engineering, Vol. 32, 2024, pp. 607-624. doi: 10.1109/TNSRE.2024.3356561

[11] S. Fakoorian, V. Azimi, M. Moosavi, H. Richter, D. Simon, "Ground Reaction Force Estimation in Pros-

thetic Legs with Nonlinear Kalman Filtering Methods", Journal of Dynamic Systems, Measurement and Control, Transactions of the ASME, Vol. 139, No. 11, 2017. doi: 10.1115/1.4036546

[12] V. Azimi, T. T. Nguyen, M. Sharifi, S. A. Fakoorian, D. Simon, "Robust Ground Reaction Force Estimation and Control of Lower-Limb Prostheses: Theory and Simulation", IEEE Transactions on Systems, Man, and Cybernetics: Systems, Vol. 50, No. 8, 2020, pp. 3024-3035. doi: 10.1109/TSMC.2018.2836913

[13] S. M. Moosavi, S. A. Fakoorian, V. Azimi, H. Richter, D. Simon, "Derivative-free Kalman filtering-based control of prosthetic legs", Proceedings of the American Control Conference, Seattle, WA, USA, 24-26 May 2017, pp. 5205-5210. doi: 10.23919/ACC.2017.7963763

[14] R. Boucetta, W. Abdallah, S. B. H. Ali, "An Adaptive Control for the Path Tracking of an Active Leg Prosthesis", International Journal of Robotics and Control Systems, Vol. 1, No. 2, 2021, pp. 159-176. doi: 10.31763/ijrcs.v1i2.350

[15] M. A. Salman, S. K. Kadhim, "Comparative Between Backstepping and Adaptive Backstepping Control for Controlling Prosthetic Knee", Iraqi Journal of Computers, Communications, Control and Systems Engineering, Vol. 23, No. 1, 2023, pp. 10. doi: 10.33103/uot.ijccce.23.1.10

[16] A. J. Peixoto, A. M. R. Ignacio De, M. F. Dos Reis, "Prosthetic legs output feedback control via variable high gain observer", Proceedings of the American Control Conference, Philadelphia, PA, USA, 10-12 July 2019, pp. 1102-1107. doi: 10.23919/ACC.2019.8814749

[17] M. Pi, "Concurrent Adaptive Control for a Robotic Leg Prosthesis via a Neuromuscular-Force-Based Impedance Method and Human-in-the-Loop Optimization", Applied Sciences, Vol. 15, No. 15, 2025. doi: 10.3390/app15158126

[18] R. Pérez-Ubeda, R. Zotovic-Stanisic, S. C. Gutiérrez, "Force Control Improvement in Collaborative Robots through Theory Analysis and Experimental Endorsement", Applied Sciences, Vol. 10, No. 12, 2020, p. 4329. doi: 10.3390/app10124329

[19] Y. Yang, D. Huang, X. Dong, "Enhanced neural network control of lower limb rehabilitation exoskeleton by add-on repetitive learning", Neurocomputing, Vol. 323, 2019, pp. 256-264. doi: 10.1016/j.neucom.2018.09.085

[20] S. Long, X. Dang, S. Sun, Y. Wang, M. Gui, "A Novel Sliding Mode Momentum Observer for Collaborative Robot Collision Detection", Machines, Vol. 10, No. 9, 2022, p. 818. doi: 10.3390/machines10090818

[21] C. Li, F. Liu, Y. Wang, M. Buss, "Concurrent Learning-Based Adaptive Control of an Uncertain Robot Manipulator With Guaranteed Safety and Performance", IEEE Transactions on Systems, Man, and Cybernetics: Systems, Vol. 52, No. 5, 2022, pp. 3299-3313. doi: 10.1109/TSMC.2021.3064971

[22] J. Kennedy, R. Eberhart, "Particle swarm optimization", Proceedings of the International Conference on Neural Networks, Perth, WA, Australia, 27 November - 1 December 1995, pp. 1942-1948. doi: 10.1109/ICNN.1995.488968

[23] A. I. Abdulkareem, A. J. Humaidi, S. M. Mahdi, "Improving the Tracking Performance of Par-4 Robot Using Nature-Inspired Optimization Algorithms to Tune the PID Controller", Iraqi Journal of Computers, Communications, Control and Systems Engineering, Vol. 26, No. 1, 2026, pp. 101-116. doi: 10.33103/2617-3352.1520

[24] A. Humaidi, Z. Waheed, "Whale optimization algorithm enhances the performance of knee-exoskeleton system controlled by smc", Iraqi Journal of Computers, Communications, Control and Systems Engineering, Vol. 23, No. 2, 2023, p. 10. doi: 10.33103/uot.ijccce.23.2.10

[25] A. J. Humaidi, I. K. Ibraheem, A. T. Azar, M. E. Sadiq, "A New Adaptive Synergetic Control Design for Single Link Robot Arm Actuated by Pneumatic Muscles", Entropy, Vol. 22, No. 7, 2020, p. 723. doi: 10.3390/e22070723

[26] B. Horsak, D. Slijepcevic, A. M. Raberger, C. Schwab, M. Worisch, M. Zeppelzauer, "GaitRec, a large-scale ground reaction force dataset of healthy and impaired gait", Scientific Data, Vol. 7, No. 1, 2020, p. 143. doi: 10.1038/s41597-020-0481-z